ELSEVIER

Controlled-release fertilizers from phosphate glass-matrix: A new ecological approach to match nutrients release with plants demand

Tariq Labbilta [a],[*],[1], Mohamed Ait-El-Mokhtar [b],[c],[d],[1], Mohamed Anli [c],[d], Abderrahim Boutasknit [c],[d], Younes Abouliatim [e], Mehdi Khouloud [f], Abdelilah Meddich [c],[d], Mohamed Mesnaoui [a],[g]

[a] Laboratory of Materials Sciences and Processes Optimization, Chemistry of Condensed Matter and Environment Team, Chemistry Department, Faculty of Sciences Semlalia, Cadi Ayyad University, Marrakech, Morocco

[b] Laboratory of Biochemistry, Environment & Agri-Food (LBEA) URAC 36, Department of Biology, Faculty of Sciences and Techniques Mohammedia, Hassan II University, Casablanca, Mohammedia, Morocco

[c] Center of Agrobiotechnology and Bioengineering, Research Unit labeled CNRST (Centre AgroBiotech-URL-CNRST-05), "Physiology of abiotic stresses team", Cadi Ayyad University, Marrakech, Morocco

[d] Laboratory of Agro-Foods, Biotechnologies, and Valorization of Bioressources Vegetales, Faculty of Science Semlalia, Cadi Ayyad University, Marrakech, Morocco

[e] Laboratory of Process and Environmental Engineering (L.I.P.E), Higher School of Technology of Casablanca, Hassan II University, Casablanca, Morocco

[f] Fertilizers Unit, Chemical & Biochemical Sciences – Green Process Engineering, Mohammed VI Polytechnic University – OCP Group, Jorf Lasfar, Morocco

[g] Center of Excellence in Soil and Fertilizer Research in Africa (CESFRA), AgroBioSciences, Mohammed VI Polytechnic University, Ben Guerir, Morocco

ARTICLE INFO

ABSTRACT

Physico-chemical properties, structural characterization, and dissolution behaviors of four phosphate glasses modified by incorporating zinc, boron, and copper, acting as eco-friendly fertilizers with controlled release of macro and micronutrients for wheat plants, were investigated. The elaborated glasses were characterized by differential thermal analysis, density measurements, X-ray diffraction, FTIR spectroscopy, and Raman spectroscopy. The dissolution behaviors were investigated using weight and pH measurements. The ionic concentration of leachate solutions was determined using ICP-OES. Results proved that the glass's chemical composition and lattice structure play the mean role in controlling the release of nutrients from the glass. The seemingly different properties between the elaborated glasses depend on the strength's bonds of glass lattice-formers and modifiers as well as their ionic field strength of the incorporated elements. An agronomic valorization was carried out to evaluate the efficiency of these agriglasses on wheat crops. It revealed a positive impact on wheat growth, yield, photosynthetic parameters, and grain mineral content

* Corresponding author.
E-mail address: tariq.labbilta@gmail.com (T. Labbilta).
[1] These authors contributed equally to this work.

with improvement values ranging from 4 to 89% compared to conventional fertilizers. These results pave the way to applying these fertilizers in large-scale experimentation to confirm their potentiality in crop production and as eco-friendly fertilizers.

Fertilizantes de liberación controlada a partir de una matriz vítrea de fosfato: un nuevo enfoque ecológico para adaptar la liberación de nutrientes a la demanda de las plantas

R E S U M E N

Palabras clave:
Fosfato
Vidrio
Durabilidad química
Trigo
Crecimiento
Rendimiento
Triticum durum

Se investigaron las propiedades fisicoquímicas, la caracterización estructural y el comportamiento de disolución de cuatro vidrios de fosfato modificados mediante la incorporación de zinc, boro y cobre, que actúan como fertilizantes ecológicos con liberación controlada de macro y micronutrientes para las plantas de trigo. Los vidrios elaborados se caracterizaron mediante análisis térmico diferencial, mediciones de densidad, difracción de rayos X, espectroscopia FTIR y espectroscopia Raman. Los comportamientos de disolución se investigaron mediante mediciones de peso y pH. La concentración iónica de las soluciones de lixiviado se determinó mediante ICP-OES. Los resultados demostraron que la composición química del vidrio y la estructura de la red juegan un papel importante en el control de la liberación de nutrientes del vidrio. Las propiedades aparentemente diferentes entre los vidrios elaborados dependen de la fuerza de los enlaces formadores de redes de vidrio y de los modificadores, así como de la fuerza del campo iónico de los elementos incorporados. Se llevó a cabo una valorización agronómica para evaluar la eficacia de estos fertilizantes en el cultivo de trigo. Reveló un impacto positivo el crecimiento del trigo, el rendimiento, los parámetros fotosintéticos y el contenido mineral del grano, con valores de mejora que van del 4 al 89% en comparación con los fertilizantes convencionales. Estos resultados allanan el camino para aplicar estos fertilizantes en la experimentación a gran escala para confirmar su potencialidad en la producción de cultivos y como fertilizantes ecológicos.

Introduction

Although the United Nations forecasts estimate that the population living on the planet is expected to increase by 2 billion by 2050, from 7.8 to 9.7 billion [1], the arable land per person is declining dramatically; the area of arable land available will have decreased by 25% in 2050 compared to 1960 according to research carried out by the National Institute for Agronomic Research [2]. This inequality requires an increase in agricultural productivity through the use of fertilizers to meet the nutritional needs of a growing population [3]. In this sense, intensive agriculture uses fertilizers and pesticides to ensure the need for nutrients and control plant diseases, and improve yields. The unbalanced use of fertilizers results in a decrease in nutrient utilization efficiency and can have a negative impact on natural ecosystems [4–6]. Generally, an "ideal" fertilizer must release nutrients only based on the plant's demand, depending on its phenological stage. It must maintain the availability of these elements throughout the growing season and beyond. Controlled-release fertilizers, especially vitreous fertilizers, are promising "green technologies" to support global food security and limit the environmental risks

related to the misuse of conventional fertilizers. Faced with the population explosion and the reduction in the area of agricultural land, the use of this category of fertilizer is starting to have attention [7]. Vitreous fertilizers ensure nutrient mobilization according to plants' specific needs during their development cycle, which promotes their optimal growth [8].

Phosphate glass is very appealing for controlled release systems due to its low chemical durability, which can be engineered to have a wide solubility range, from a few hours to several years, by adjusting its composition, which leads to structural changes [9,10]. Phosphate glasses' chemical durability also relies on the field strength, charge, and size of the modifier cation incorporated within the glass matrix [11].

Otherwise, wheat is an essential crop with many purposes due to its widespread use as human and animal feed [12,13]. In this context and in order to sustain food security, improving wheat production is currently regarded as a significant challenge around the world [14,15]. Wheat productivity in Morocco and other North African countries is hampered by a variety of abiotic and biotic stresses, including high temperatures, drought, soil poverty in organic and mineral matter, leaf rust, and altered soil physical characteristics, particularly the decline of cropland resources, which is already severely
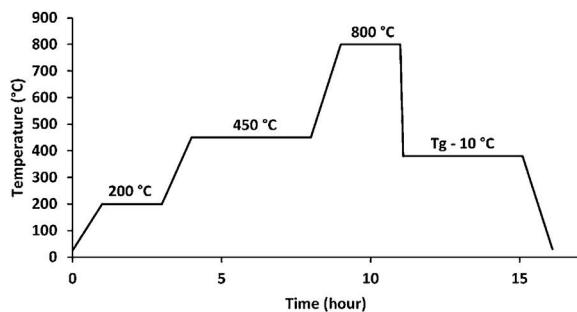
Fig. 1 – Thermal profile used to elaborate glasses.

restricting crop yields in these countries [16–18]. Morocco's wheat production is estimated to be 2,561,898 tons in 2020, with an arable area of 2,845,290 hectares. Morocco imported 5,848,817 tons of wheat in the same year to meet its needs, making it the world's 10th largest grain importer, up 48.2% from 2019 [19].

Several studies have been reported on the use of phosphate glass as a controlled fertilizer. These studies usually lack extensive information on degradation behavior. They are usually restricted to a single glass system, relatively high melting temperatures, low microelement uptake, and fairly a modest agronomic study limited to a simple description of the growth parameters. According to wheat nutrient requirements, four phosphate glass formulations (AGF0–AGF1–AGF2–AGF3) were developed in this study: AGF0 contains just primary and secondary nutrients (P_2O_5-K_2O-CaO-MgO), AGF1 and AGF2 contain zinc and boron, respectively, while AGF3 has copper. The influence of these elements on physicochemical qualities (density and molar volume), glass structure, thermal properties, and dissolving behavior were investigated in order to determine their potential for use as controlled-release fertilizers. Agronomic valorization was also carried out in the greenhouse to evaluate the agronomic potential of the selected agriglass fertilizers on wheat growth, yield, photosynthesis, grain mineral content, and soil physicochemical parameters.

Materials and methods

Glass synthesis

The melt quenching process was used to make the glass samples, which included as starting materials $CaCO_3$, K_2CO_3, $NH_4H_2PO_4$, MgO, ZnO, H_3BO_3, and CuO. The batch components were precisely weighed, finely ground, and fully mixed in an agate mortar before being deposited in an alumina crucible. To avoid $NH_4H_2PO_4$ foam and to remove CO_2, NH_3, and H_2O from the decomposition of the starting components, the batches were cooked for 2 h at 200 °C and 4 h at 450 °C. Fig. 1 shows these steps in addition to the melting step, which lasted 2 h at 800 °C [20].

The melted liquids were taken out of the furnace and poured onto a carbon mold to cool in the air. All of the samples were annealed for 4 h at 10 °C below their transition temperature before being progressively cooled to room temperature.

The final glass compositions were determined using inductively coupled optical emission spectroscopy (ICP-OES Ultima Expert, Horiba Inc., Ontario, Canada).

To validate the glasses' amorphous nature, an X-ray diffraction examination was performed (with a PANAanalytical XPERT diffractometer operating at 40 kV/200 mA, the angular range 10°–70°(2) was scanned with a step size of 0.07°(2) and a counting time of 5 s/step).

Thermal analysis

The thermal properties of glass samples were determined using a thermal analyzer (STA PT 1600, Linseis, Germany). Temperatures of the glass transition (T_g), the onset of crystallization ($T_{c,on}$), and the melting (T_m) were determined in an alumina crucible by heating samples at a rate of 10 °C min^{-1} from ambient temperature to 800 °C. Glass stability against crystallization is indicated by a value, K_H, according to Hruby [21]. $K_H = (T_{c,on} - T_g)/(T_{liq} - T_{c,on})$ is the formulae for this parameter. Glasses with higher K_H values, according to Hruby, have better stability against crystallization on heating and, presumably, better vitrifiability on cooling.

Density measurements

At room temperature, the density of the glass was evaluated using the Archimedes technique with diethyl-ortho-phthalate as the buoyant liquid. The density of the glass was determined using the conventional buoyancy test technique (ASTM C693). The mass of the glass sample was evaluated both in air and after immersion in diethyl-ortho-phthalate. The density was determined using the following equation [22]:

$$\rho_{glass} = \frac{W_{glass}}{W_{glass} + (W_{ortho} - W_{(ortho+glass)})} \times \rho_{ortho}$$

with: ρ_{glass} = glass density; W_{glass} = weight of glass measured in air; W_{ortho} = weight of diethyl-ortho-phthalate only; $W_{ortho+glass}$ = weight of glass immersed in diethyl-ortho-phthalate; ρ_{ortho}: diethyl-ortho-phthalate density = 1.11422 g/cm^3.

The measurements were performed three times to get an average density value.

The molar volume (V_M) was obtained using the equation from the density data and molecular glass weight of the batch composition: $V_M = \rho_{glass/Mglass}$ with M_{glass} as the glass's molar mass [23].

Characterization of glass structure

The structure of the glass was analyzed using Fourier transform infrared spectroscopy and Raman spectroscopy. FTIR spectra in the 400–4000 cm^{-1} region were acquired using the KBr method on a Bruker VERTEX 70 spectrometer with a resolution of 4 cm^{-1} and 32 scans per determination. Glass fine powder samples were mixed in a ratio of (0.01/0.99 g) with KBr.

The Raman spectrum was obtained by examining glass powder with the Confotec MR520 Raman Confocal Microscope. An Ar ion laser's 514 nm line was employed as the excitation source. The spectra were collected in the 400–4000 cm^{-1} range

Table 1 – The applied treatments and their description.	
Treatment	Description
Control	Treatment with no fertilizer addition
NPK fertilizer	Treatment with traditional chemical fertilizers
AGF1 D1	Treatment with formulae 1 of agriglass fertilizers applied at 0.3 g/pot
AGF1 D1 + N	Treatment with formulae 1 of agriglass fertilizers applied at 0.3 g/pot with chemical nitrogen supplementation (1.4 g N/pot)
AGF1 D2	Treatment with formulae 1 of agriglass fertilizers applied at 1 g/pot
AGF1 D2 + N	Treatment with formulae 1 of agriglass fertilizers applied at 1 g/pot with chemical nitrogen supplementation (1.4 g N/pot)
AGF2 D1	Treatment with formulae 2 of agriglass fertilizers applied at 0.3 g/pot
AGF2 D1 + N	Treatment with formulae 2 of agriglass fertilizers applied at 0.3 g/pot with chemical nitrogen supplementation (1.4 g N/pot)
AGF2 D2	Treatment with formulae 2 of agriglass fertilizers applied at 1 g/pot
AGF2 D2 + N	Treatment with formulae 2 of agriglass fertilizers applied at 1 g/pot with chemical nitrogen supplementation (1.4 g N/pot)
AGF3 D1	Treatment with formulae 3 of agriglass fertilizers applied at 0.3 g/pot
AGF3 D1 + N	Treatment with formulae 3 of agriglass fertilizers applied at 0.3 g/pot with chemical nitrogen supplementation (1.4 g N/pot)
AGF3 D2	Treatment with formulae 3 of agriglass fertilizers applied at 1 g/pot
AGF3 D2 + N	Treatment with formulae 3 of agriglass fertilizers applied at 1 g/pot with chemical nitrogen supplementation (1.4 g N/pot)

using a 10-objective and a 1-s exposure time in the micro-Raman compartment.

Glass dissolution

The glasses were ground in a ball mill (Pulverisette 6, Fritsch, France) and then sieved through two sieves with varied mesh sizes of 1 and 2 mm. To evaluate their chemical stability, 1 g of glass powder was added to a flask holding 20 mL of distilled water. The initial pH value of the solution is 6.5. Ten samples of each composition were made and placed in a thermostatic bath set to 25 °C to measure the rate of release for a period ranging from 1 to 35 days.

The solution was filtered and the pH was determined using an Adwa AD8000 digital pH meter. After drying the residual glass at 90 °C for 10 h, it was weighed using an analytical balance with a sensitivity of 0.1 mg (Shimadzu AW220). The following formulae was used to get the percentage of weight reduction [24]:

$$D_R = \frac{W_i - W_t}{W_i} \times 100$$

where W_i and W_t represent the initial and final weights of the sample.

The ionic concentration of leachate solutions was determined using inductively coupled optical emission spectroscopy.

Evaluation of the glass fertilizers agronomic potential

Plant material and experimental design
To assess the effect of the prepared glass fertilizers (GF) on wheat performances, a pot experiment was performed in the greenhouse with a 25.5 °C temperature average, 68.5% relative humidity average, a day/night cycle of 16/8 h, and 410 m^{-2} s^{-1} photon flux density average. The experiment lasted from 18 January 2021 to 8 May 2021. The agronomic valorization was performed for the AGF1, AGF2, and AGF3 formula, whereas the AGF0 formulae was already performed in a previous study [24]. The experiment was carried out using two doses of the obtained glass fertilizers (AGF D1 = 0.3 and AGF D2 = 1 g/plant) and a recommended dose of conventional chemical fertilizer

(NPK) (140 kg N ha^{-1} as ammonium nitrate + 80 kg P$_2$O$_5$ ha^{-1} as superphosphate + 50 kg K$_2$O ha^{-1} as potassium sulfate) [25].

The substrate used in this experiment was a field soil sampled from the district of Saada (10 km Southwest of Marrakesh, Morocco). The soil physicochemical parameters are as follow: sand, 51%; loam, 30%; clay, 19%; pH, 7.92; electrical conductivity (EC), 1.72 mS cm^{-1}; total organic carbon, 0.80%; organic matter, 1.3% and available phosphorus, 31 mg kg^{-1}.

Wheat (*Triticum durum* L. cv. Carioca) seeds were sterilized for 10 min by immersion in a 10% sodium hypochlorite solution and then rinsed five times with sterile distilled water. Seeds germination was carried out in plastic dishes containing a sterile filter paper disk with incubation for seven days at 28 °C in the dark. One week after germination (day 0 of sowing), seedlings were transplanted into 2 L plastic pots (1 seedling and 1.9 kg of soil/pot) with the application of the different treatments.

In this experiment, 14 treatments were applied as described in Table 1. The chemical nitrogen supplementations were performed by adding ammonium nitrate. Ten replicates for each treatment were randomly disposed for a total of 140 pots. Pots irrigation was performed twice a week with the same amount of distilled water to maintain a field capacity of about 75%.

Growth parameters
After four months from germination (110 days after sowing), plants were harvested, and growth and yield traits were measured, including plant height, root length, leaf area, number of leaves, ears, shoot and root dry weight, weight and number of grains, and the weight of 1000 grain. Dry weight measurements were recorded after the plant samples were kept at 105 °C for 24 h.

Stomatal conductance and photosynthetic efficiency
Fully expanded leaves from the same rank were used for stomatal conductance and photosynthetic efficiency measurements, where five plants were used for each treatment.

The stomatal conductance measurements (g_s) were recorded on a sunny day before harvest (108 days after sowing) using a porometer system (Leaf Porometer LP1989, Decagon Device, Inc., Washington, DC, USA).
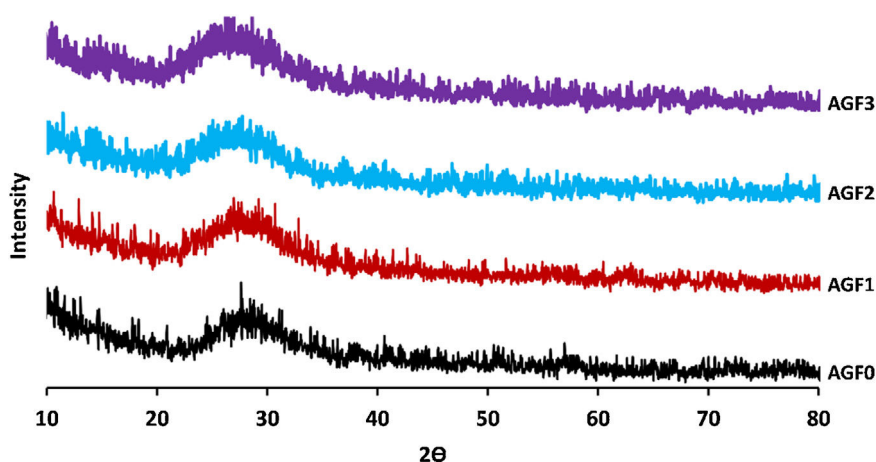
Fig. 2 – XRD patterns for AGF0, AGF1, AGF2 and AGF3 glasses.

Photosynthetic efficiency values were obtained using a portable fluorometer (Optisciences OSI 30p). Leaves were kept in the dark for 30 min using leaf clips, and then the measurements were recorded. Photosynthetic efficiency was evaluated as F_v/F_m ratio where $F_v = F_m - F_0$ and F_m and F_0 are maximum and initial fluorescence, respectively [26].

Soil analyses and wheat grain mineral content

Soil samples were collected, for each treatment, before and after the experiment. The determination of soil texture was carried out following the Robinson protocol [27]. Samples pH and EC were determined using a 1:5 (w:v) aqueous solution. Soil and wheat grain mineral content was measured according to Segarra [28]. Dried material (50 mg) was digested in 1 mL of HNO_3, 0.6 mL of H_2O_2, and 1 mL of deionized water for 48 h at 90 °C. Then, the mixture was diluted using deionized water (10 mL final volume). N, P, K, Mg, Ca, Fe, Mn, Zn, B, and Cu concentrations were measured using inductively coupled plasma-atomic emission spectroscopy (ICP-OES).

Statistical analysis

Data were presented as mean values based on three to five replicates ±standard error (SE). Statistical analysis was performed using SPSS software (IBM Corp. Released 2013. IBM SPSS Statistics for Windows, Version 22.0. Armonk, NY, USA: IBM Corp.) package for Windows. One-way analysis of variance (ANOVA) as performed for all data and the differences among means were assessed using Student–Newman–Keuls (SNK) test calculated at $p < 0.05$.

Results and discussion

Glass formation

The XRD patterns of all samples support their amorphous nature, as shown in Fig. 2, there is no sharp peak in the diffraction patterns [29]. The entire surface of the glasses was stable and homogeneous.

Few bubbles were observed, and all the obtained glasses were transparent. AGF0, AGF1, and AGF2 were colorless, while AGF3 was blue. The blue color of AGF3 phosphate glass suggested the presence of Cu^{2+} ions [30]. The analyzed compositions of the studied glasses (Table 2). For all glasses, there were some modest discrepancies between nominal and measured compositions, which can be attributable to measurement errors and volatilization during the heating treatment.

Thermal behavior

Table 3 lists the temperatures for the glass transition (T_g), onset crystallization ($T_{c,on}$), and melting (T_m) acquired from DTA curves for the prepared glasses. The thermal properties of glass AGF3 are similar to those of glass AGF0, indicating that the amount of CuO included in the glass matrix had no effect. Because of the ionic field strength of zinc and boron (IFS = z/r^2, where z is the valence cation and r is the ionic radius), glass AGF2 has greater values of T_g, $T_{c,on}$, and T_m than glass AGF1, being IFS equal to 0.59 for Zn and 1.34 for B, according to Dietzel [31]. The increase in the thermal properties, especially T_g values, which is determined by the amount and strength of cross-links between the cation and oxygen atoms, as well as the density of covalent cross-linking, is critical for understanding the physical characteristics of glasses. This augmentation in T_g indicates that the structure is becoming stronger and the lattice is becoming more stable [32]. Furthermore, it has been found that ZnO-based glasses have a low glass transition temperature among the large class of phosphate glasses [33]. With this in mind, it was projected that adding ZnO to the glass formulation would have no significant effect on the glass's thermal properties.

As demonstrated in Table 2, adding microelements to the phosphate glass matrix raised K_H from 0.319 for AGF0 to 0.445, 0.447, and 0.35 for AGF1, AGF2, and AGF3 glasses, respectively. Because the presence of these oxides enhances the lattice by establishing cross-links between phosphate chains, the thermal stability of the examined glasses is higher than that of the microelements-free glass sample [32].

Table 2 – Nominal and analyzed compositions of the studied glasses.

Glass code	Nominal composition (% mol)							Analyzed composition (% mol)						
	P_2O_5	K_2O	CaO	MgO	ZnO	B_2O_3	CuO	P_2O_5	K_2O	CaO	MgO	ZnO	B_2O_3	CuO
AGF0	50	33.34	11.11	5.55	0	0	0	50.17 ± 0.35	33.26 ± 0.23	11.07 ± 0.07	5.50 ± 0.04	0.00	0.00	0.00
AGF1	50	33.12	11.03	5.51	0.34	0	0	49.92 ± 0.35	33.34 ± 0.23	10.98 ± 0.07	5.44 ± 0.04	0.32 ± 0.01	0.00	0.00
AGF2	49.92	33.28	11.09	5.55	0	0.16	0	49.80 ± 0.35	33.14 ± 0.23	11.13 ± 0.07	5.76 ± 0.04	0.00	0.17 ± 0.01	0.00
AGF3	50	33.26	11.09	5.54	0	0	0.11	49.95 ± 0.35	33.14 ± 0.23	11.11 ± 0.07	5.70 ± 0.04	0.00	0.00	0.10 ± 0.01

Table 3 – Glass transition (T_g) crystallization ($T_{c,on}$) melting (T_m) temperatures, K_H, density, and molar volume (V_M) of prepared glasses.

Glass code	T_g (°C)	$T_{c,on}$ (°C)	T_m (°C)	K_H	Density (g cm^{-3})	M_V (mol cm^{-3})
AGF0	340 ± 2	417 ± 5	658 ± 3	0.32 ± 0.01	3.341 ± 0.002	33.185 ± 0.19
AGF1	342 ± 2	442 ± 3	662 ± 4	0.44 ± 0.01	3.362 ± 0.003	32.979 ± 0.31
AGF2	349 ± 3	449 ± 1	673 ± 3	0.45 ± 0.01	3.342 ± 0.003	33.154 ± 0.25
AGF3	339 ± 3	421 ± 4	656 ± 2	0.35 ± 0.01	3.353 ± 0.004	33.066 ± 0.35

Glass density and molar volume

The measured densities and computed molar volumes of the examined glasses are summarized in Table 3. Glass density changes could indicate the vitreous lattice's structural compactness; it is sensitive to spatial arrangement and atom nature [34,35]. However, because most of the microelements introduced are glass modifiers (except for B_2O_3), and are mostly concentrated in the holes in the glass lattice, these modifications were modest and unlikely to be significant in this study. Molar volume, which measures the volume filled by a single mole of glass, is more sensitive to changes in the glass structure than density. It normalizes the atomic masses of glass constituents [23]. By integrating microelements, the molar volume decreases, indicating that the glass structure becomes more compact [32]. Furthermore, the decrease in V_M followed by an increase in T_g most likely represents an overall increase in glassy matrix cross-linking [36]. The regular decrease in the molar volume for the manufactured glasses is strongly related to the kind of bending in the glass structure, because P–O–X (X = Zn, B, or Cu) bridges are more ionic than P–O–P bridges, implying the vitreous lattice's compactness. However, because boron has a greater IFS than zinc, it was expected that the M_V of AGF2 glass would be lower than AGF1 glass. Nonetheless, since B_2O_3 is a lattice forming, the molar volume numbers may not always accurately represent the true compactness inside the glass structure [37].

Glass structure

Fig. 3 shows the Raman spectra of the four phosphate glasses in the frequency range of 200 to 1400 cm^{-1}. The phosphate lattice is made up of phosphate tetrahedral units, which are characterized by the number of bridging oxygen atoms per tetrahedron using the Q^n terminology, where n indicates the number of bridging oxygen atoms per tetrahedron (n = 0, 1, 2, 3) [38].

All Raman spectra showed strong features around 1160 and 690 cm^{-1}, which can be deconvoluted using Gaussian lines to recover additional component bands, as illustrated in Fig. 3. Around 1270, 1090, 700, and 320–400 cm^{-1}, other weaker features can be seen. The band at roughly 1320 cm^{-1} is assigned to the symmetric stretching of the (P=O) bond in Q^3 groups [39,40]. The asymmetric stretching of (O–P–O) in the Q^2 groups, $V_{as}(PO_2^-)$, occurs around 1270 cm^{-1} [41].

The symmetric stretching vibration of (O–P–O) in the Q^2 groups, $V_s(PO_2^-)$, is responsible for the most intense peak at approximately 1160 cm^{-1} [41]. The symmetric stretching vibration of terminal (PO_3^{2-}) units in the Q^1 groups is attributable to a shoulder that appeared at 1160 cm^{-1} and was displayed by deconvolution [42]. The symmetric stretching vibration of (P–O–P) in the Q^1 groups, v_s(P–O–P), is related to another shoulder by nearly 730 cm^{-1}, as determined by deconvolution [43]. The peak at 690 cm^{-1} is caused by the symmetric stretching vibration of Q^2 groups (P–O–P), while the weak feature at 640 cm^{-1} is caused by symmetric stretching vibrations in Q° orthophosphate units (v_s (P–O), Q°) [44]. The antisymmetric P–O bond in (P_2O_7) groups (Q^1) could be represented by a weak feature of about 525 cm^{-1} [22,45]. The bending vibrations of PO_2^- and PO_3^{2-} are involved in the wide peaks between 320 and 400 cm^{-1} [40].

The FTIR spectra for glassware samples between 400 and 1400 cm^{-1} are shown in Fig. 4. The FTIR spectra of the four formulations showed no significant differences, indicating that the produced glasses have identical chemical functional groups and chemical bonding. The two non-bridging oxygen atoms connected to a phosphorus atom in the phosphate tetrahedron Q^2 are responsible for the band at around 1280 cm^{-1} (PO_2^-). The symmetric stretch of (O–P–O) in Q^2 groups is characterized by the vibrations of the bands detected at 1160 cm^{-1}. The stretching vibrations v_s PO_3^{2-} in the phosphate tetrahedron Q^1 are assigned to the FTIR band around 1090–1100 cm^{-1}, whereas the stretching vibrations as O–P–O in the phosphate tetrahedron Q^1 are assigned to the band around 960–1050 cm^{-1}. Asymmetric and symmetric stretching of the bridging oxygen atoms bound to a phosphorus atom in a Q^2 phosphate tetrahedron are responsible for the two absorption peaks at 880 and 720 cm^{-1}, respectively. The band about 770 cm^{-1}, on the other hand, is related to the P–O–P stretching vibrations in various PO_4 tetrahedra (Q^1 species). The bending vibration of O–P–O and PO_3^{2-} bonds is related to bands that emerge between 550 and 490 cm^{-1} [22,33,46]. Table 4 summarizes the frequency ranges and assignments of the Raman and infrared bands of the examined glasses.
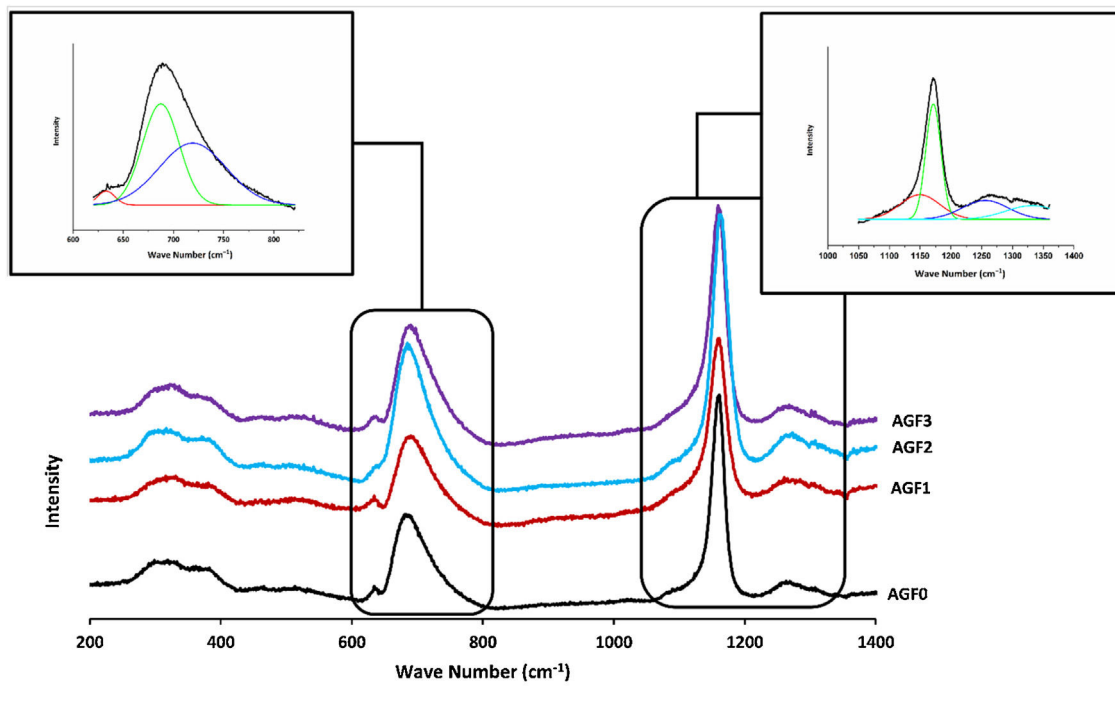
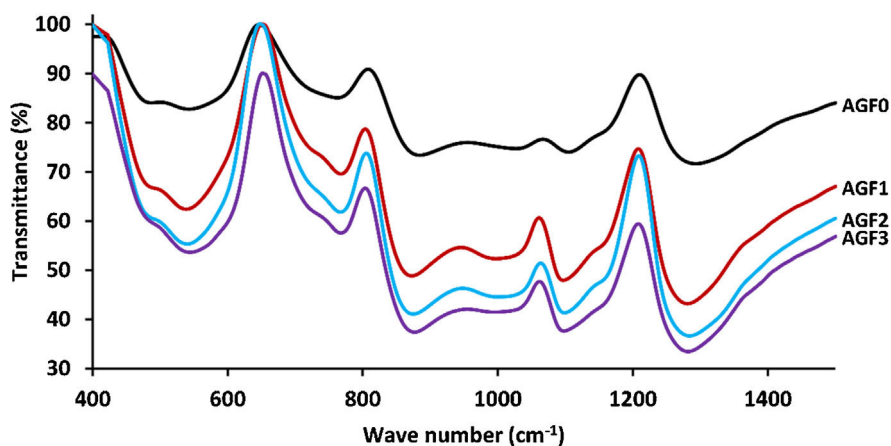**Fig. 3 – Raman spectra of AGF0, AGF1, AGF2, and AGF3 glasses.**

Fig. 4 – FTIR spectra of AGF0, AGF1, AGF2, and AGF3 glasses. Raman and FTIR spectra suggest that the structure of the phosphate lattice approaches metaphosphates, and the lattice is based mainly on Q^2 units. However, the spectra also show the existence of Q^1 units, which generally result in shorter phosphate chains.

Dissolution behavior

As the degradation time in distilled water extended, the glasses showed an increasing dissolution rate (measured by percent of weight loss), as shown in Fig. 5. Chemical bonds are formed between glass formers and glass modifiers during the vitrification process. Consequently, those modifiers cannot be released if the glass remains undissolved.
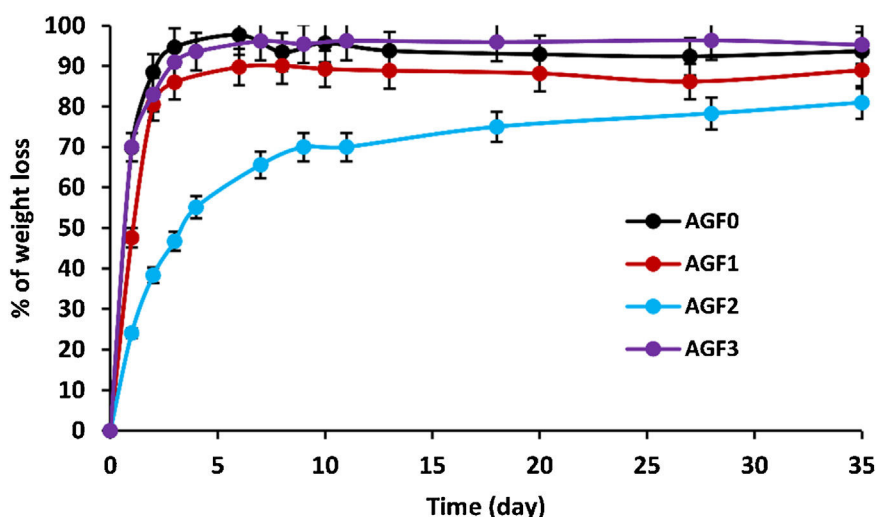
Glass dissolution is a complicated process that is influenced by its intrinsic qualities as well as the leaching conditions [47]. Interdiffusion, ion exchange, reaction-diffusion, and hydrolysis occur when the glass comes into contact with water. Three dissolution rate regimes are involved in these

processes: (i) Initial diffusion, which reflects the interaction of glass lattice-modifier cations and protons in the solution. Water species penetrate the glass at the start of dissolution, and protons in the solution undergo diffusional ion exchange with mobile alkali modifier ions; (ii) Hydrolysis process, which involves the hydrolysis of P–O–M bonds (M = P, Mg, Ca, B, Zn, Cu, etc.) that constitute the glass' net structure [48]. Hydrolysis alters the phosphate lattice by breaking bridging bonds formed in the interphase as a result of the release of mobile elements; (iii) rate drop and residual rate is a transition between the initial and residual dissolution rates due to the solution's progressive saturation. This saturation causes the rate of glass dissolution to gradually decrease until it achieves

Table 4 – Frequency ranges (cm^{-1}) and assignments of the Raman and infrared bands of the studied glasses.

								Assignment
				Wave number (cm^{-1})				
AGF0		AGF1		AGF2		AGF3		
FTIR	Raman	FTIR	Raman	FTIR	Raman	FTIR	Raman	
–	1318	–	1326	–	1323	–	1314	V_s (P=O), Q^3
1296	1270	1284	1268	1284	1274	1282	1265	V_{as} (PO$_2^-$), Q^2
1159	1161	1155	1161	1155	1166	1159	1159	V_s (PO$_2^-$), Q^2
1107	1092	1097	1096	1101	1100	1099	1088	V_s (PO$_3^{2-}$), Q^1
962–1074	–	987–1031	–	995–1051	–	987–1033	–	V_{as} (PO$_2^-$), Q^1
885	–	875	–	877	–	879	–	V_{as} (P–O–P), Q^2
761	730	769	733	767	736	769	730	V_s (P–O–P), Q^1
717	691	727	696	729	689	724	694	V_s (P–O–P), Q^2
–	640	–	639	–	642	–	642	V_s (P–O), Q$^\circ$
–	527	–	526	–	523	–	525	(P$_2$O$_7$)$^{4-}$ groups, Q^1
557	386	544	385	543	388	549	384	δ(PO$_2^-$)
487	324	487	325	484	329	487	326	δ(PO$_3^{2-}$)

Abbreviations: δ, bending; V: stretching; s: symmetric; as: asymmetric.

Fig. 5 – The trend of weight loss of AGF0, AGF1, AGF2, and AGF3 glasses.

Table 5 – The initial dissolution rate of AGF0, AGF1, AGF2, and AGF3 glasses.

Glass code	AGF0	AGF1	AGF2	AGF3
V_0 (g/day)	0.69	0.47	0.24	0.70

a relatively constant amount (residual dissolution rate); the chemical affinity for dissolution decreases [47,48] – i.e., thermodynamic equilibrium is approached.

Table 5 shows the initial dissolving rates V_0, which are computed from the slope of the linear approximation $V_0 = am/dt$ of the dissolution curves. The chemical resistance of glass is mostly determined by its composition. The highest dissolving rates were found in formula AGF0 and AGF3, whereas the lowest dissolution rate was found in formulae AGF2, which included boron oxide, followed by AGF1. With an initial dissolution rate of $V_0 = 0.7$ g/day, the first diffusion and hydrolysis process for AGF0 and AGF3 lasted only two days. In less than five days, almost the whole glass lattice was dissolved in water.

By integrating zinc and boron into the glass matrix, the degradation rate of AGF1 and AGF2 was reduced. These glasses have initial dissolving rates of 0.47 and 0.24 g/day, respectively. The first diffusion and hydrolysis process took three to six days to complete.

ZnO is an intermediate oxide. Depending on its content in the phosphate lattice, it can behave as a former or modifier lattice. ZnO oxide acts as a glass former when it occupies tetrahedral sites by generating ZnO$_4$ structural units. However, when a small amount of Zn is present (which is the case in our study), it fills the coordinated octahedral positions, and ZnO oxide functions as a glass modifier [49]. The formation of the P–O–Zn ionic bond, which induces an increase in the compactness and rigidity of the glass lattice, is expected to improve the chemical stability of the structure as well as the thermal properties of phosphate glasses when ZnO is added to the glass lattice [50]. However, this increase was not too remarkable given that the added amount of ZnO (according to the needs of the wheat) was low. Therefore the number of P–O–Zn bonds formed led to
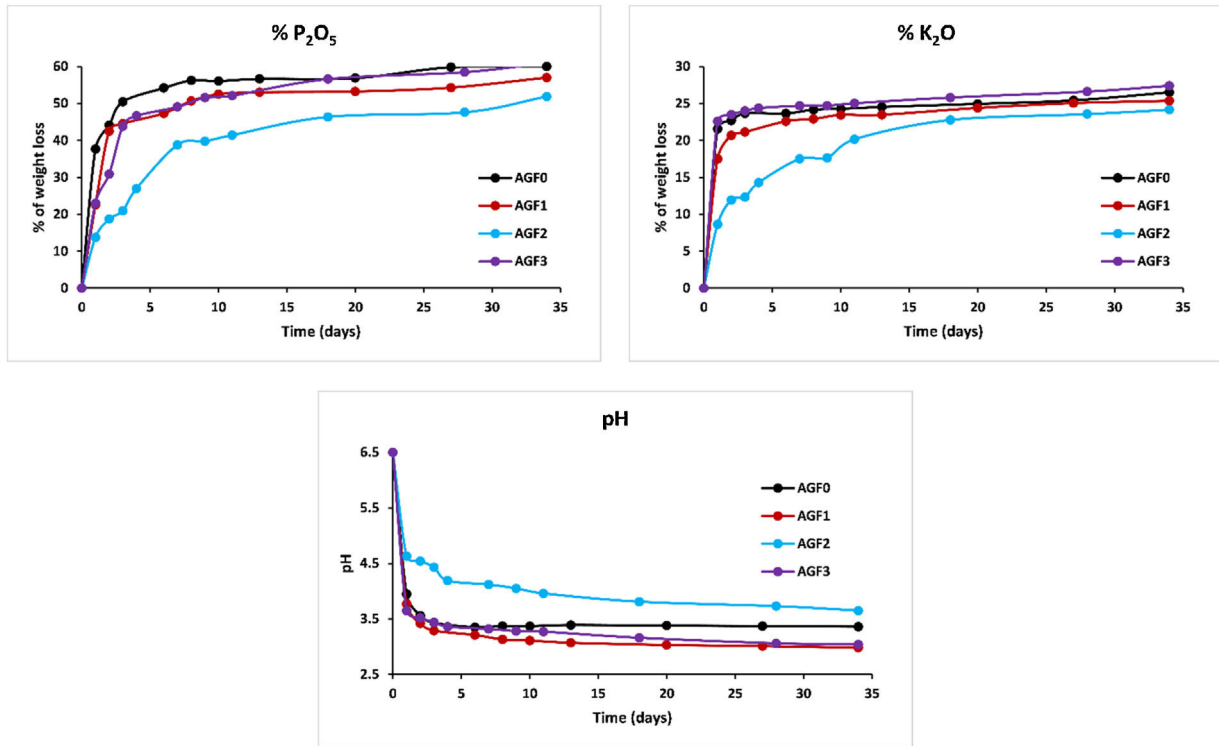
Fig. 6 – Percentage of glass constituents (macro-elements) analyzed in the leachate solutions (elements in the form of oxides) normalized to the initial glass weight and pH measurements versus time for AGF0, AGF1, AGF2, and AGF3.
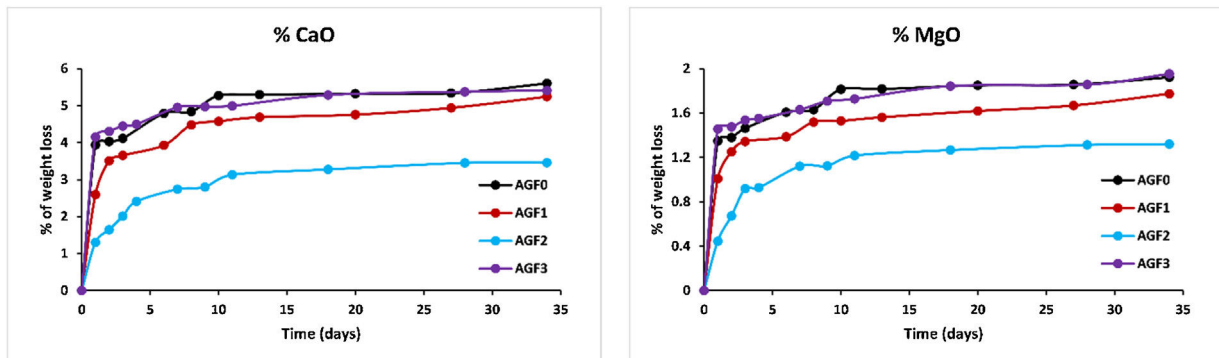

Fig. 7 – Percentage of glass constituents (secondary elements) analyzed in the leachate solutions (elements in the form of oxides) normalized to the initial glass weight versus time for AGF0, AGF1, AGF2, and AGF3.

a slight increase in the chemical durability of our phosphate glasses.

A decrease of almost 30% in the weight loss and initial dissolution rate was observed in the dissolution behavior of the glass containing B_2O_3 glasses over 35 days as compared to the glasses with no microelements. The creation of P–O–B bonds, which related well to an increase in transition temperature, caused a decrease in the percentage of weight loss and dissolution rate with the addition of B_2O_3. The chemical bond strength of the diatomic molecule B–O (808 kJ/mol) is higher than that of the diatomic molecule P–O (599.1 kJ/mol), implying an energetic preference for stronger bonding forces inside the glass structure via the production of P–O–B bonds [51]. Shah et al. [52] noticed that the dissolution rate slowed as the B_2O_3 level increased while examining the dissolution

of phosphate glasses in the Na_2O–BaO–B_2O_3–P_2O_5 quaternary system.

Previous studies indicated an increase in the chemical stability of phosphate glasses by incorporating copper oxide, which was corroborated by an increase in density and glass transition temperature [53]. However, in this study, and since copper is one of the microelements which are consumed in minimal quantities by the plant (with molybdenum and silica), it is incorporated, within the vitreous lattice, in a negligible amount compared to the other elements (calcium, magnesium), which limited its effect and made it unobservable whether on thermal properties, on density and molar volume, or the chemical stability.

Figs. 6–8 show the amounts of cations released from the studied glasses in the form of oxides, normalized to the
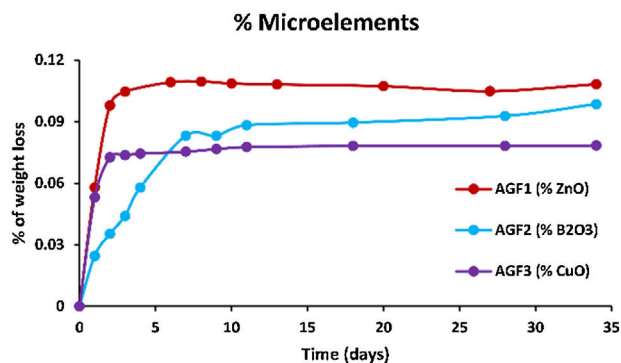
Fig. 8 – Percentage of glass constituents (micro-elements) analyzed in the leachate solutions (elements in the form of oxides) normalized to the initial glass weight versus time for AGF1, AGF2, and AGF3.

starting glass weight, as measured by the ICP-OES method, as well as the pH readings. The percentage of released ions increased over time. For AGF0 and AGF3, concentrations of constituent cations in distilled water increased dramatically during the first two days of immersion (although the determination of copper in the dissolving solution was difficult since it was incorporated in small amounts). While for glasses AGF1 and AGF2, the effect of the addition of microelements, which results in a slower release of ions in water, has been noted. For all the studied glasses, the presence of entire cations in the leachate solution, with a ratio equivalent to the glass composition, suggests that no selective leaching occurred, and the glasses dissolved congruently instead [54]. Congruent dissolution can reflect that the dissolution mechanism is based on a release of the entire metaphosphates chain in solution; this chain contains all the incorporated elements linked in covalent bonds to oxygens. After immersing the glasses in distilled water, the pH of the leachate solutions dropped. The pH of all glasses decreased linearly with immersion time from 6.5 to reach the acidic region, then remained nearly constant for the duration of immersion. Previous research has found that the pH of the leachate solution varies depending on the phosphate content of the immersed glass, with more phosphorus concentration in the solution resulting in lower pH values [48].

Soil analysis

The NPK and glass fertilizers application showed a significant decrease in soil pH compared to the control, while electrical conductivity recorded a considerable increase (Table 6). Soils supplemented with glass fertilizers also showed a significant decline in pH value compared to conventional fertilizers, where AGR3 D2 recorded the greatest decrease (13%). This result corroborates our findings related to the dissolution of the glass fertilizers in the water, inducing a significant decrease in pH values. A previous study [55] indicated that soil supplementation with glass and conventional fertilizers induced a small lowering in soil pH. In this investigation, even if the different fertilizers significantly decreased soil pH, their values remain slightly alkaline, which indicates no evident effect of the applied fertilizers on this parameter. Moreover,

soil electrical conductivity showed significant variations after the application of the glass fertilizers compared to the NPK treatment since AGF2 D2 recorded the maximum decrease (49%) while AGF3 D1 + N recorded the greatest enhancement (28%).

Considering soil mineral content, no significant difference was recorded between soil mineral status before the experiment and harvest for the control (Table 6). The application of different fertilizers mainly induced an increment in soil mineral content compared to the control except for Ca and Fe concentration, where a decreasing trend was recorded. When compared to NPK fertilizer, AGF1 mainly improved P, K, B, and Cu content (296%, 208%, 64%, and 25%, respectively), AGF3 mainly improved N, Mg, Ca, and Mn content (5%, 43%, 14%, and 49%, respectively), while AGF2 mainly improved Zn content (105%). A recent study reported the application of glass fertilizers induced a declining trend in macroelements edaphic concentrations while an increasing trend was observed for microelements content [55]. In this study, the increase in soil mineral concentrations observed after the application of the glass fertilizers may be attributed to the composition of these fertilizers rich in essential mineral nutrients, especially P, K, Mg, Ca, Zn, B, and Cu and their controlled release in the soil which makes them available for the plant and limits their leaching. The same result was reported by Labbilta [24,56] reporting that the agriglass fertilizers applied to tomato and wheat improved soil mineral content compared to NPK and the control treatments.

Growth and yield parameters

The application of AGF3 treatments mainly improved shoot height, leaf area, root, ear, and grain total dry weights, the number of grains per plant, and 1000 grain weight, while AGF2 formulations mainly enhanced root elongation and shoot dry weight in comparison to the control and NPK treatments (Table 7). The same result was recently reported by Labbilta et al. [24] showing the boosting effect of the application of three phosphate glass fertilizers formula ($P_2O_5 + K_2O + CaO + MgO + Fe_2O_3$, $P_2O_5 + K_2O + CaO + MgO + MnO$ and $P_2O_5 + K_2O + CaO + MgO + Fe_2O_3 + MnO + ZnO + B_2O_3 + CuO + MoO_3$) on wheat growth performance and yield under greenhouse conditions with an increase of up to 88% compared to the control and NPK treated plants. The same authors [56] indicated the same positive impact of these fertilizers on tomato under field conditions. Furthermore, previous studies reported an improvement in tomato yield after the application of glass fertilizers under field conditions compared to conventional fertilizers [55,57]. In the same vein, Ouis et al. [11] and Abou-Baker et al. [58] reported the same beneficial effect of SiO_2, P_2O_5, and K_2O-based glass fertilizers on maize ears, straw, and grains weights and yield.

The positive impact of the elaborated glass fertilizers on wheat growth performance and yield could be attributed to their richness in essential mineral elements [58,59]. Ait-El-Mokhtar et al. [60] reported the greatest values of wheat growth and yield traits in the field after the application of three phosphate glass fertilizers supplemented with chemical nitrogen. In this study, no obvious significant effect was recorded

Table 6 – Soil physicochemical characteristics before and after the cultivation of wheat treated with agriglass and chemical fertilizers.

	Fertilizer treatment	Texture	pH	EC (mS cm^{-1})	N (mg/kg)	P (mg/kg)	K (mg/kg)	Ca (mg/kg)	Mg (mg/kg)	Fe (mg/kg)	Mn (mg/kg)	Zn (mg/kg)	B (mg/kg)	Cu (mg/kg)
Before the experiment		Sandy-silty-clayey	8.60 ± 0.14[b]	0.19 ± 0.01[h]	443.67 ± 38.68[def]	52.87 ± 3.35[g]	0.30 ± 0.03[h]	12.66 ± 0.58[a]	1.96 ± 0.08[e]	2.33 ± 0.58[e]	7.39 ± 0.34[g]	0.41 ± 0.16[d]	1.37 ± 0.32[a]	0.97 ± 0.03[b]
	Control		8.88 ± 0.20[a]	0.25 ± 0.08[gh]	395.67 ± 17.89[f]	35.93 ± 2.54[i]	0.33 ± 0.03[gh]	9.45 ± 0.22[de]	2.50 ± 0.35[d]	5.81 ± 0.17[a]	9.65 ± 0.56[f]	0.83 ± 0.02[c]	0.62 ± 0.07[cd]	1.20 ± 0.17[ab]
	NPK fertilizer		8.43 ± 0.03[bc]	0.67 ± 0.11[d]	522.17 ± 21.36[c]	26.87 ± 1.85[j]	0.34 ± 0.03[gh]	10.37 ± 0.11[c]	2.47 ± 0.15[d]	5.90 ± 0.09[a]	8.62 ± 0.33[f]	0.94 ± 0.05[c]	0.59 ± 0.10[d]	1.23 ± 0.13[ab]
After the experiment	AGF1 D1		8.42 ± 0.42[bc]	0.34 ± 0.11[fgh]	442.23 ± 18.47[def]	66.33 ± 2.89[f]	1.04 ± 0.05[b]	8.34 ± 0.64[f]	3.12 ± 0.09[c]	4.88 ± 0.10[bc]	10.80 ± 0.69[e]	1.88 ± 0.33[b]	0.81 ± 0.08[bcd]	1.09 ± 0.08[b]
	AGF1 D1 + N		7.64 ± 0.11[gh]	0.94 ± 0.08[c]	433.77 ± 19.63[def]	110.00 ± 3.46[f]	1.36 ± 0.06[a]	9.00 ± 0.26[def]	3.68 ± 0.08[b]	5.33 ± 0.58[ab]	4.15 ± 0.73[h]	1.19 ± 0.27[c]	1.06 ± 0.05[abc]	1.18 ± 0.16[ab]
	AGF1 D2		7.93 ± 0.14[ef]	0.99 ± 0.16[c]	559.45 ± 21.94[c]	108.67 ± 4.04[d]	1.09 ± 0.07[b]	9.35 ± 0.30[de]	4.13 ± 0.11[a]	4.15 ± 0.13[d]	13.53 ± 0.46[b]	1.11 ± 0.33[c]	0.83 ± 0.14[bcd]	1.86 ± 0.12[a]
	AGF1 D2 + N		8.02 ± 0.14[def]	0.38 ± 0.09[efg]	567.07 ± 19.63[c]	140.33 ± 4.62[c]	0.70 ± 0.05[d]	8.62 ± 0.54[ef]	3.10 ± 0.09[c]	5.73 ± 0.23[a]	11.60 ± 0.52[de]	1.95 ± 0.05[b]	1.14 ± 0.22[ab]	1.63 ± 0.32[ab]
	AGF2 D1		8.10 ± 0.06[de]	0.67 ± 0.03[d]	457.68 ± 7.50[d]	55.07 ± 2.54[g]	0.34 ± 0.04[gh]	9.11 ± 0.10[def]	2.68 ± 0.19[d]	5.11 ± 0.09[abc]	8.55 ± 0.47[f]	1.08 ± 0.07[c]	0.74 ± 0.22[bcd]	1.09 ± 0.08[b]
	AGF2 D1 + N		7.75 ± 0.18[fg]	0.89 ± 0.20[c]	402.63 ± 14.43[ef]	83.80 ± 4.16[e]	0.93 ± 0.03[c]	8.75 ± 0.21[def]	2.65 ± 0.13[d]	5.63 ± 0.32[a]	11.93 ± 0.81[cd]	1.89 ± 0.10[b]	0.73 ± 0.24[bcd]	1.56 ± 0.38[ab]
	AGF2 D2		8.29 ± 0.08[cd]	0.49 ± 0.04[def]	545.44 ± 37.53[c]	85.67 ± 4.04[e]	0.53 ± 0.04[e]	10.33 ± 0.29[c]	3.18 ± 0.08[c]	5.63 ± 0.32[a]	12.87 ± 0.75[bc]	1.95 ± 0.05[b]	0.52 ± 0.10[d]	1.30 ± 0.26[ab]
	AGF2 D2 + N		7.86 ± 0.02[f]	0.34 ± 0.01[fgh]	436.09 ± 2.89[def]	163.00 ± 6.93[a]	0.76 ± 0.04[d]	8.86 ± 0.12[def]	3.39 ± 0.25[bc]	5.71 ± 0.25[a]	8.96 ± 0.03[f]	2.79 ± 0.18[a]	0.57 ± 0.11[d]	1.58 ± 0.36[ab]
	AGF3 D1		7.84 ± 0.05[f]	0.85 ± 0.01[cd]	647.12 ± 8.08[b]	44.67 ± 4.04[h]	0.41 ± 0.02[fg]	11.86 ± 0.11[b]	2.76 ± 0.14[d]	4.57 ± 0.37[cd]	13.53 ± 0.46[b]	1.07 ± 0.06[c]	0.67 ± 0.20[cd]	1.21 ± 0.18[ab]
	AGF3 D1 + N		7.84 ± 0.05[f]	0.57 ± 0.00[d]	755.60 ± 18.47[a]	108.00 ± 5.20[d]	0.87 ± 0.05[c]	10.93 ± 0.06[c]	4.11 ± 0.10[a]	5.82 ± 0.16[a]	15.67 ± 0.58[a]	1.25 ± 0.22[c]	0.92 ± 0.07[bcd]	1.61 ± 0.33[ab]
	AGF3 D2		7.92 ± 0.01[ef]	0.66 ± 0.20[d]	449.34 ± 16.16[de]	90.87 ± 3.35[e]	0.44 ± 0.04[f]	9.66 ± 0.58[d]	3.59 ± 0.16[b]	4.23 ± 0.20[d]	12.40 ± 0.35[bcd]	1.11 ± 0.09[c]	0.68 ± 0.19[cd]	1.19 ± 0.16[ab]
	AGF3 D2 + N		7.31 ± 0.30[i]	0.80 ± 0.01[cd]	336.00 ± 12.12[g]	151.00 ± 8.66[b]	0.89 ± 0.04[c]	9.17 ± 0.14[def]	3.73 ± 0.20[b]	5.24 ± 0.21[ab]	9.78 ± 0.19[f]	1.17 ± 0.29[c]	0.89 ± 0.10[bcd]	1.51 ± 0.43[ab]

Table 7 – Effects of the agriglass fertilizers on the growth, yield, and photosynthetic parameters of wheat after 4 months of cultivation.

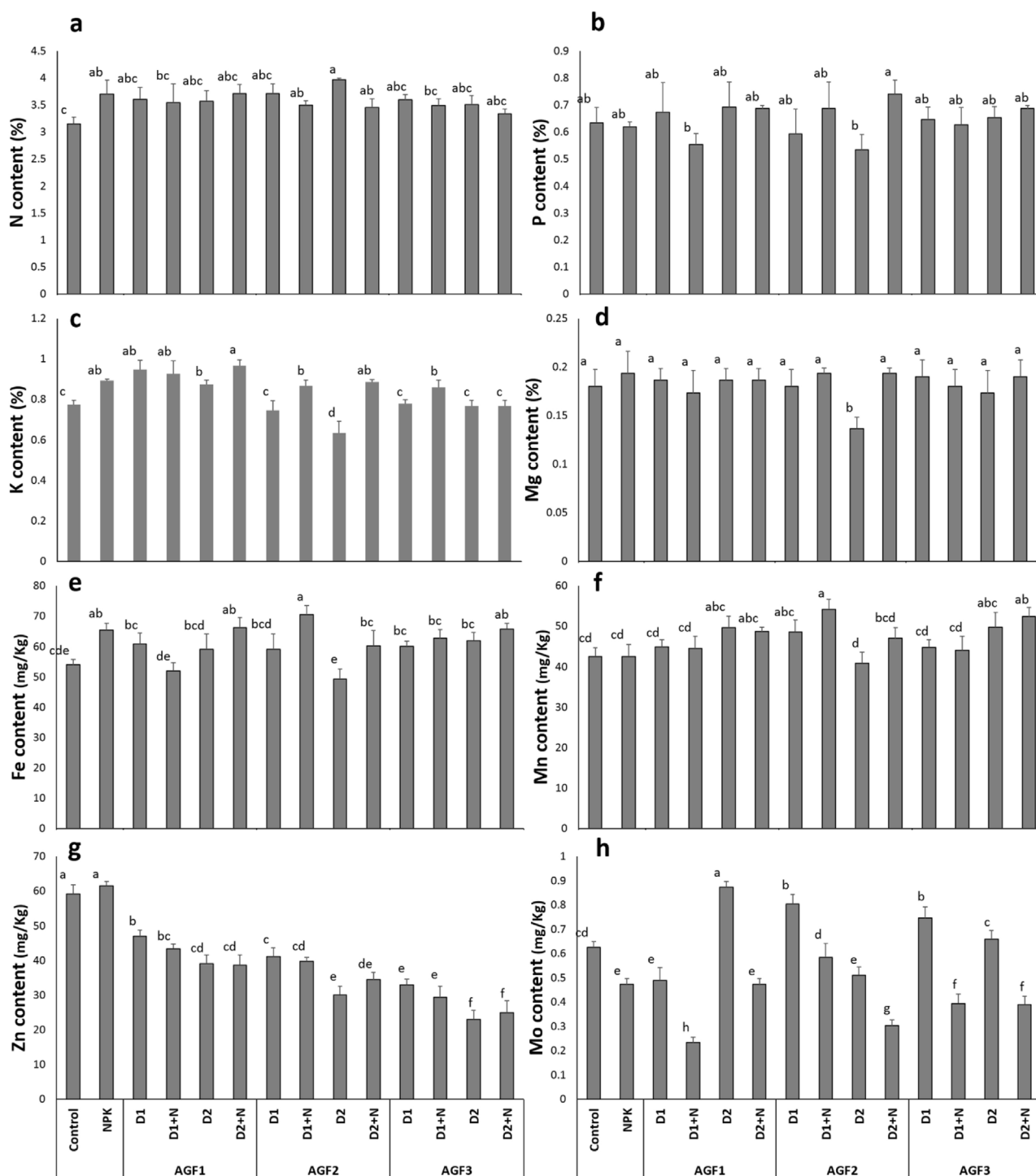| Fertilizer treatment	Plant height (cm)	Root length (cm)	Number of leaves	Leaf area (cm^2)	Shoot dry weight (g)	Root dry weight (g)	Ear dry weight (g)	Total grain weight/plant (g)	Number of grain/plant	1000 grain weight (g)	Stomatal conductance (mmol m^{-2} s^{-1})	F_v/F_m
Control	62.30 ± 4.20[c]	16.67 ± 1.53[b]	6.003 ± 1.00[a]	18.52 ± 1.30[e]	0.93 ± 0.11[c]	0.42 ± 0.05[e]	1.07 ± 0.25[e]	0.66 ± 0.12[c]	25.00 ± 6.56[b]	23.86 ± 0.70[e]	16.93 ± 2.32[d]	0.67 ± 0.05[c]
NPK fertilizer	68.10 ± 1.65[bc]	20.33 ± 2.31[ab]	7.67 ± 1.15[a]	29.40 ± 2.60[cd]	1.32 ± 0.19[bc]	0.39 ± 0.06[e]	1.42 ± 0.20[e]	1.05 ± 0.28[bc]	38.67 ± 8.50[ab]	27.05 ± 2.45[de]	23.87 ± 3.11[cd]	0.75 ± 0.03[abc]
AGF1 D1	86.13 ± 2.22[a]	24.67 ± 2.08[ab]	7.00 ± 1.00[a]	27.99 ± 2.66[cd]	2.05 ± 0.26[a]	0.56 ± 0.07[cde]	2.24 ± 0.07[a–d]	1.67 ± 0.17[ab]	50.00 ± 9.16[a]	37.98 ± 1.31[bcd]	26.50 ± 4.23[c]	0.78 ± 0.03[abc]
AGF1 D1 + N	76.27 ± 3.85[ab]	26.67 ± 2.08[a]	7.33 ± 1.53[a]	28.15 ± 2.51[cd]	1.86 ± 0.28[ab]	0.50 ± 0.07[de]	2.11 ± 0.32[bcd]	1.42 ± 0.31[ab]	45.67 ± 14.57[a]	33.19 ± 2.91[bcd]	23.37 ± 3.39[cd]	0.72 ± 0.05[abc]
AGF1 D2	75.83 ± 3.82[ab]	29.00 ± 3.46[a]	6.670 ± 1.15[a]	26.39 ± 4.06[cd]	1.83 ± 0.20[ab]	0.46 ± 0.05[de]	2.12 ± 0.36[bcd]	1.46 ± 0.30[ab]	47.00 ± 9.16[a]	33.50 ± 1.13[bcd]	23.50 ± 2.19[cd]	0.73 ± 0.05[abc]
AGF1 D2 + N	84.97 ± 4.46[a]	21.67 ± 2.89[ab]	6.33 ± 0.58[a]	40.35 ± 2.86[a]	2.22 ± 0.52[a]	0.79 ± 0.18[abc]	2.34 ± 0.14[a–d]	1.57 ± 0.14[ab]	50.33 ± 3.05[a]	35.06 ± 4.33[bcd]	26.27 ± 2.61[c]	0.73 ± 0.05[abc]
AGF2 D1	79.33 ± 6.71[ab]	25.17 ± 2.47[ab]	7.33 ± 1.53[a]	31.94 ± 5.26[a–d]	2.55 ± 0.38[a]	0.92 ± 0.14[a]	1.91 ± 0.17[d]	1.06 ± 0.13[bc]	39.00 ± 3.60[ab]	28.84 ± 0.77[cde]	30.23 ± 2.58[bc]	0.73 ± 0.04[abc]
AGF2 D1 + N	77.57 ± 2567[ab]	24.33 ± 3.05[ab]	6.67 ± 1.15[a]	23.61 ± 1.65[de]	1.82 ± 0.27[ab]	0.61 ± 0.09[cde]	2.13 ± 0.19[bcd]	1.44 ± 0.11[ab]	46.33 ± 2.08[a]	30.98 ± 1.31[cde]	26.07 ± 2.69[c]	0.69 ± 0.01[bc]
AGF2 D2	82.90 ± 6.72[a]	29.33 ± 7.09[a]	6.33 ± 0.58[a]	35.69 ± 2.27[abc]	2.32 ± 0.37[a]	0.50 ± 0.08[de]	2.38 ± 0.16[a–d]	1.56 ± 0.14[ab]	41.33 ± 4.04[ab]	43.74 ± 6.95[a]	28.03 ± 1.76[c]	0.76 ± 0.03[abc]
AGF2 D2 + N	86.83 ± 4.54[a]	25.67 ± 3.79[ab]	6.67 ± 0.58[a]	38.93 ± 2.57[ab]	1.99 ± 0.19[ab]	0.48 ± 0.05[de]	1.99 ± 0.13[cd]	1.18 ± 0.08[b]	40.33 ± 2.52[ab]	33.06 ± 6.01[bcd]	24.07 ± 3.46[cd]	0.80 ± 0.02[ab]
AGF3 D1	73.10 ± 6.05[ab]	20.00 ± 4.36[ab]	7.00 ± 1.00[a]	31.48 ± 5.72[a–d]	1.82 ± 0.14[ab]	0.69 ± 0.05[bcd]	2.27 ± 0.28[a–d]	1.61 ± 0.21[ab]	51.67 ± 10.50[a]	32.64 ± 1.73[bcd]	29.60 ± 2.19[bc]	0.74 ± 0.01[abc]
AGF3 D1 + N	82.20 ± 6.36[a]	24.00 ± 4.00[ab]	7.67 ± 1.15[a]	30.49 ± 4.78[bcd]	2.15 ± 0.20[a]	0.73 ± 0.07[abc]	2.60 ± 0.18[ab]	1.81 ± 0.16[a]	53.33 ± 3.21[a]	36.15 ± 1.39[abc]	36.63 ± 3.19[b]	0.69 ± 0.07[abc]
AGF3 D2	84.87 ± 2.87[a]	27.00 ± 2.00[a]	6.67 ± 0.58[a]	32.97 ± 4.57[a–d]	1.87 ± 0.24[ab]	0.69 ± 0.09[bcd]	2.57 ± 0.09[abc]	1.79 ± 0.06[a]	48.00 ± 10.39[a]	41.72 ± 1.19[ab]	42.37 ± 3.81[a]	0.76 ± 0.05[abc]
AGF3 D2 + N	86.10 ± 4.03[a]	28.67 ± 1.53[a]	8.00 ± 1.00[a]	34.13 ± 2.44[abc]	1.87 ± 0.08[ab]	0.85 ± 0.04[ab]	2.67 ± 0.19[ab]	1.92 ± 0.32[a]	48.33 ± 4.16[a]	40.34 ± 2.57[ab]	30.87 ± 6.26[bc]	0.84 ± 0.06[a]

Fig. 9 – Fruit mineral content ((a) nitrogen, (b) phosphorus, (c) potassium, (d) magnesium, (e) iron, (f) manganese, (g) zinc, and (h) molybdenum) of wheat plants treated with glass and chemical fertilizers. Bars with different letters are significantly different according to the SNK test, after performing one-way ANOVA (P < 0.05).

on wheat growth, yield, and physiological performances after the application of chemical nitrogen which could be attributed to the fact that this element was leached with the irrigation in contrast to the other elements that are present in the glass fertilizer. This result is confirmed by the modest values of soil nitrogen recorded after N supplementation which are mainly

close to the value obtained before the experiment except for AGF1 D2 + N and AGF3 D1 + N treatments.

When considering the growth-promoting effect of the applied glass fertilizers in comparison to NPK fertilizers, it appears that AGF3 recorded the greatest effect on wheat growth fitness and yield, followed by AGF2 and AGF1. The high

boosting effect of AGF3 may be explained by the dissolution rate of this glass in comparison the other two formula of glass fertilizers since it recorded the greatest dissolution values for P_2O_5, K_2O, CaO, and MgO, which provide a sufficient amount of macroelement to the plant. These phosphate glass fertilizers supply a significant amount of phosphorus, potassium, calcium, and magnesium to plants. Increased shoot and root biomass accumulation, as well as fruit and seed formation, were associated with improved nutrient uptake [61,62].

Photosynthetic parameters

The application of NPK fertilizer enhanced stomatal conductance (g_s) by 41% and photosystem II efficiency (F_v/F_m) by 12% in comparison to the control. In addition, the glass fertilizers treated plants showed an increase of gs by 21% (8% for AGF1, 16% for AGF2, and 39% for AGF3) compared to the NPK treatment (Table 7), while F_v/F_m showed fluctuations between the different AGF and recorded the greatest increment (7%) with the application of AGF3 D1 + N in comparison to NPK fertilizer. Labbilta et al. [24,56] reported the same positive effect of the application of glass fertilizers on these photosynthetic parameters on wheat and tomato under greenhouse and field conditions, respectively.

The promotion of gs and Fv/Fm in the glass fertilizers treated plants could be linked in the first place to the pivotal role mineral nutrients released by these amendments such as K, Mg, Cu, Fe, and Mn known to be a part of the photosynthetic apparatus and functioning. Labbilta et al. [56] reported the improvement of these elements' concentration in soil supplemented with phosphate glass fertilizers which may contribute to the stimulation of photosynthesis activity after their absorption. A previous study [63] indicated an increased nutrient status in grapevine treated with the glass fertilizers, especially potassium and magnesium uptake, which may boost photosynthetic activity and metabolism pathways, including stomatal opening, chlorophyll biosynthesis, and multiple key enzymes involved in carbon dioxide assimilation as well as the regulation of abscisic acid production [64]. On the other hand, AGF3 induced the maximum increase of these parameters (78% (AGF3 D2) for gs and 7% (AGF3 D1 + N) for Fv/Fm) in comparison to the NPK treatment. The distinguished effect of this formulae could be attributed to the speed of nutrient release (including K, Mg, Cu), which was more important for AGF3 compared to AGF2 and AGF1.

Grain mineral content

Results in Fig. 9 indicate that the application of NPK treatment showed a significant improvement in N, K, and Fe grain mineral concentration (18%, 16%, and 21%, respectively) in comparison to the control. Moreover, the NPK amendment caused a 24% decline in Mo concentration while no significant differences were noticed in P and Mg, Mn, and Zn content in comparison to the untreated wheat. The glass fertilizers application recorded almost the same effect of NPK treatment on these parameters except for Zn concentration, where a decreasing trend was noticed compared to the NPK and control and Mo content which showed improved

values when the glass fertilizers were applied without N supplementation. The greatest increase (84%) in wheat grain mineral content was recorded for Mo concentration after the application of AGF1 D2 treatment in comparison to the NPK treatment. Our results are in line with the findings of previous studies [56,63] reporting the improvement of grain or fruit mineral content compared to the control. Indeed, Labbilta et al. [56] noticed that tomato fruit showed an improved mineral content with the application of agriglass fertilizers under field conditions. The positive effect of the phosphate glass fertilizers on wheat grain mineral content could be explained by the improved availability of these elements in the rhizospheric soil, which fit the plants' needs in a timing fashion.

Conclusions

The physicochemical properties, structure, and dissolution behaviors of four phosphate glasses were examined in this study in relation to wheat nutrient requirements. The studied glasses were proven to be amorphous, and Raman and FTIR spectra revealed that the phosphate lattice's structure approaches that of metaphosphates, with the lattice-based primarily on Q^2 units. With the addition of various components such as B_2O_3 and ZnO, the glass transition temperature (T_g), onset crystallization temperature ($T_{c,on}$), melting temperature (T_m), and glass stability increased, while the molar volume (V_M) and glass dissolution decreased. These behaviors are thought to be caused by phosphate chain cross-linking and the replacement of the weakly hydrated P–O–P bond with a more chemically resistant X–O–P bond (X = Zn, B). In contrast, incorporating a small amount of copper oxide had no significant effect on the glass's physicochemical properties.

Moreover, all glasses dissolved congruently, and no selective ion leaching was observed. The agronomic valorization of the obtained glass fertilizers revealed a positive impact on wheat growth fitness, yield, photosynthetic parameters, and grain mineral content compared to conventional fertilizers and to the control. These results pave the way to applying these fertilizers in large-scale experimentation to confirm their potentiality in crop production and as an eco-friendly fertilizer.

Conflicts of interest

The authors declare no conflict of interest.

Mohammed VI Polytechnic University, National Center of Scientific and Technical Research CNRST, Ministry of Higher Education, Scientific Research and Professional Training of Morocco MESRSFC) under the project entitled *Elaboration et caractérisation de nouveaux engrais vitrifiés à base des phosphates*, project ID *VAL-MES-01/2017*.

We thank our sponsors who provided insight, expertise, and follow-up that greatly assisted this research.

REFERENCES

[1] D.D. Wrachien, B. Schultz, M.B. Goli, Impacts of population growth and climate change on food production and irrigation and drainage needs: a world-wide view, Irrig. Drain 70 (2021) 981–995, http://dx.doi.org/10.1002/ird.2597.

[2] INRA – AgriMaroc. Available online: https://www.agrimaroc.ma/terres-arables-diminuer/ (accessed 29.12.21).

[3] J. Bruinsma, World Agriculture: Towards 2015/2030: An FAO Perspective, 1st ed., Earthscan, London, 2003, http://dx.doi.org/10.4324/9781315083858.

[4] P. Prashar, S. Shah, Impact of fertilizers and pesticides on soil microflora in agriculture, Sustain. Agric. Rev. 576 (2016) 331–361, http://dx.doi.org/10.1007/978-3-319-26777-7_8.

[5] T. Adhikari, R.C. Gowda, R.H. Wanjari, M. Singh, Impact of continuous fertilization on heavy metals content in soil and food grains under 25 years of long-term fertilizer experiment, Commun. Soil Sci. Plant Anal. 52 (2021) 389–405, http://dx.doi.org/10.1080/00103624.2020.1854290.

[6] T. Garnett, M.C. Appleby, A. Balmford, I.J. Bateman, T.G. Benton, P. Bloomer, B. Burlingame, M. Dawkins, L. Dolan, D. Fraser, M. Herrero, I. Hoffmann, P. Smith, P.K. Thornton, C. Toulmin, S.J. Vermeulen, H.C.J. Godfray, Sustainable intensification in agriculture: premises and policies, Science 341 (2013) 33–34, http://dx.doi.org/10.1126/science.12344.

[7] A.E. Al-Rawajfeh, M.R. Alrbaihat, E.M. AlShamaileh, Characteristics and types of slow- and controlled-release fertilizers, in: F.B. Lewu, V. Tatiana, T. Sabu, K.R. Rakhimol (Eds.), Controlled Release Fertilizers for Sustainable Agriculture, 2nd ed., Academic Press, Cambridge, Massachusetts, 2020, pp. 57–58, http://dx.doi.org/10.1016/B978-0-12-819555-0.00004-2.

[8] T. Labbilta, L. Abielaala, M. Mesnaoui, H. Aouad, Y. Abouliatim, M. Khouloud, A. El Abiad, Controlled-release fertilizers: study of the vitrifiable system $3P_2O_5–2K_2O–(1−x)CaO–xMgO$, in: PLUMEE 2019, vol. 9, 2019, pp. 94–97.

[9] J.J. Videau, A. El Hadrami, C. Labrugère, M. Couzi, L. Montagne, M. Mesnaoui, M. Maazaz, Structural influence of alumina in Zn-Cd-Pb phosphate glasses, Phys. Chem. Glas. Eur. J. Glas. Sci. Technol. Part B 48 (2007) 363–372.

[10] L.L. Velli, C.P.E. Varsamis, E.I. Kamitsos, D. Möncke, D. Ehrt, Structural investigation of metaphosphate glasses, Phys. Chem. Glasses 46 (2005) 178–181.

[11] M.A. Ouis, M. Abd-Eladl, N.H. Abou-Baker, Evaluation of Agriglass as an environment friendly slow release fertilizer, Silicon 10 (2016) 293–299, http://dx.doi.org/10.1007/s12633-016-9443-7.

[12] S.W. Culman, S.S. Snapp, M. Ollenburger, B. Basso, L.R. DeHaan, Soil and water quality rapidly responds to the perennial grain kernza wheatgrass, J. Agron. 105 (2013) 735–744, http://dx.doi.org/10.2134/agronj2012.0273.

[13] M.R. Abdollahi, F. Zaefarian, H. Hunt, M.N. Anwar, D.G. Thomas, V. Ravindran, Wheat particle size, insoluble fibre sources and whole wheat feeding influence gizzard

[14] musculature and nutrient utilization to different extents in broiler chickens, J. Anim. Physiol. Anim. Nutr. 103 (2019) 146–161, http://dx.doi.org/10.1111/jpn.13019.

[14] T. Curtis, N.G. Halford, Food security: the challenge of increasing wheat yield and the importance of not compromising food safety, Ann. Appl. Biol. 164 (2014) 354–372, http://dx.doi.org/10.1111/aab.12108.

[15] B. Liu, P. Martre, F. Ewert, J.R. Porter, A.J. Challinor, C. Müller, A.C. Ruane, K. Waha, P.J. Thorburn, P.K. Aggarwal, M. Ahmed, Global wheat production with 1.5 and 2.0 °C above pre-industrial warming, Glob. Change Biol. 25 (2019) 1428–1444, http://dx.doi.org/10.1111/gcb.14542.

[16] S. Ren, Q. Qin, H. Ren, Contrasting wheat phenological responses to climate change in global scale, Sci. Total Environ. 15 (2019) 620–631, http://dx.doi.org/10.1016/j.scitotenv.2019.01.394.

[17] I.T. Abdelhedi, S.Z. Zouari, Agriculture and food security in North Africa: a theoretical and empirical approach, J. Knowl. Econ. 11 (2020) 193–210, http://dx.doi.org/10.1007/s13132-018-0528-y.

[18] M. Ait-El-Mokhtar, A. Boutasknit, R. Ben-Laouane, M. Anli, F. El Amerany, S. Toubali, S. Lahbouki, S. Wahbi, A. Meddich, Vulnerability of oasis agriculture to climate change in Morocco, in: M. Khosrow-Pour (Ed.), Impacts of Climate Change on Agriculture and Aquaculture, IGI Global, Hershey, 2020, pp. 76–106, http://dx.doi.org/10.4018/978-1-6684-3686-8.ch058.

[19] FAOSTAT, 2021. Available online: http://www.fao.org/faostat/en/#home (accessed 21.12.21).

[20] T. Labbilta, M. Mesnaoui, H. Aouad, Y. Abouliatim, M. Khouloud, L. Abielaala, Study of the effect of calcium substitution 587 by magnesium in the vitreous system $3P_2O_5-2K_2O-(1−x)$ CaO-x MgO, Materials 13 (2020) 2637, http://dx.doi.org/10.3390/ma13112637.

[21] A. Hruby, Evaluation of glass-forming tendency by means of DTA, Czech. J. Phys. B. 22 (1972) 1187–1193, http://dx.doi.org/10.1007/BF01690134.

[22] R. Makhlouk, N. Beloued, S. Aqdim, Study of chromium-lead-phosphate glasses by XRD, IR, density and chemical durability, Adv. Mater. Phys. Chem. 8 (2018) 269–280, http://dx.doi.org/10.4236/ampc.2018.86018.

[23] A.A. Ahmed, A.A. Ali, A. El-Fiqi, Glass-forming compositions and physicochemical properties of degradable phosphate and silver-doped phosphate glasses in the P_2O_5-CaO-Na_2O-Ag_2O system, J. Mater. Res. Technol. 8 (2019) 1003–1013, http://dx.doi.org/10.1016/j.jmrt.2018.07.012.

[24] T. Labbilta, M. Ait-El-Mokhtar, Y. Abouliatim, M. Khouloud, A. Meddich, M. Mesnaoui, Elaboration and characterization of vitreous fertilizers and study of their impact on the growth, photosynthesis and yield of wheat (*Triticum durum* L.), Materials 14 (2021) 1295, http://dx.doi.org/10.3390/ma14051295.

[25] A.C. Elalaoui, Fertilisation Minérale des Cultures: les èlèments fertilisants majeurs (N, P K), Transf. Technol. Agric. 155 (2007) 4.

[26] N.R. Baker, Chlorophyll fluorescence: a probe of photosynthesis in vivo, Annu. Rev. Plant Biol. 59 (2008) 89–113, http://dx.doi.org/10.1146/annurev.arplant.59.032607.092759.

[27] D. Baize, Guide des analyses courantes en pédologie, 3rd ed., INRA, Paris, 1988.

[28] G. Segarra, E. Casanova, C. Borrero, M. Avilés, I. Trillas, The suppressive effects of composts used as growth media against Botrytis cinerea in cucumber plants, Eur. J. Plant Pathol. 117 (2007) 393–402, http://dx.doi.org/10.1007/s10658-007-9108-x.

[29] D. Bellucci, A. Sola, R. Salvatori, A. Anesi, L. Chiarini, V. Cannillo, Role of magnesium oxide and strontium oxide as modifiers in silicate-based bioactive glasses: effects on

thermal behaviour, mechanical properties and in-vitro bioactivity, Mater. Sci. Eng. C. Mater. Biol. Appl. 72 (2008) 566–575, http://dx.doi.org/10.1016/j.msec.2016.11.110.

[30] O. Soriano-Romero, R.A. Lozada-morales, Meza. Rocha, S. Carmona-Téllez, U. Caldiño, B. Flores-Desirena, R. Palomino-Merino, Cold bluish white and blue emissions in Cu+-doped zinc phosphate glasses, J. Lumin. 217 (2020) 116791, http://dx.doi.org/10.1016/j.jlumin.2019.116791.

[31] A.Z. Dietzel, Die Kationenfeldstärken und ihre Beziehungen zu Entglasungsvorgängen, zur Verbindungsbildung und zu den Schmelzpunkten von Silicaten, Phys. Chem. Chem. Phys. 48 (2010) 9–23, http://dx.doi.org/10.1002/BBPC.19420480104.

[32] J. Schwarz, H. Tichá, L. Tichý, R. Mertens, Physical properties of PbO-ZnO-P2O5 glasses. I. Infrared and Raman spectra, J. Optoelectron. Adv. Mater. 6 (2004) 737–746.

[33] S. Nian, Y. Zhang, J. Li, N. Zhou, W. Zou, Glass formation and properties of sodium zinc phosphate glasses doped with ferric oxide, Adv. Appl. Ceram. 117 (2018) 319–327, http://dx.doi.org/10.1080/17436753.2017.1417956.

[34] K. Franks, I. Abrahams, G. Georgiou, J.C. Knowles, Investigation of thermal parameters and crytallisation in a ternary CaO-Na$_2$O-P$_2$O$_5$ based glass system, Biomaterials 22 (2000) 497–501, http://dx.doi.org/10.1016/S0142-9612(00)00207-6.

[35] R.O. Omrani, S. Krimi, J.J. Videau, I. Khattech, A. El Jazouli, M. Jemal, Structural investigations and calorimetric dissolution of manganese phosphate glasses, J. Non-Cryst. Solids 389 (2014) 66–71, http://dx.doi.org/10.1016/j.jnoncrysol.2014.02.006.

[36] M.A. Chaudhry, M. Altaf, Electrical properties of Na$_2$O-CdO-P$_2$O$_5$ glasses, Mod. Phys. Lett. B 14 (2000) 319–326, http://dx.doi.org/10.1142/S0217984900000434.

[37] D. Radu, O. Dumitrescu, I. Pincovschi, Dependence of structural compactness upon the compositional characteristics for the glasses in Na$_2$O-xAl$_2$O$_3$-65B$_2$O$_3$ system, Rom. J. Mater. 6 (2016) 530–537.

[38] A. Kiani, J.V. Hanna, S.P. King, G.J. Rees, M.E. Smith, N. Roohpour, V. Salih, J.C. Knowles, Structural characterization and physical properties of P$_2$O$_5$-CaO-Na$_2$O-TiO$_2$ glasses by Fourier transform infrared, Raman and solid-state magic angle spinning nuclear magnetic resonance spectroscopies, Acta Biomater. 8 (2012) 333–340, http://dx.doi.org/10.1016/j.actbio.2011.08.025.

[39] Y.M. Lai, X.F. Liang, S.Y. Yang, J.X. Wang, B.T. Zhang, Raman spectra study of iron phosphate glasses with sodium sulfate, J. Mol. Struct. 1013 (2012) 134–137, http://dx.doi.org/10.1016/j.molstruc.2012.01.025.

[40] A. Chahine, M. Et-Tabirou, J.L. Pascal, FTIR and Raman spectra of the Na$_2$O–CuO–Bi$_2$O$_3$-P$_2$O$_5$ glasses, Mater. Lett. 58 (2004) 2776–2780, http://dx.doi.org/10.1016/j.matlet.2004.04.010.

[41] P. Stoch, W. Szczerba, W. Bodnar, M. Ciecinska, A. Stoch, E. Burkel, Structural properties of iron-phosphate glasses: spectroscopic studies and ab initio simulations, Phys. Chem. Chem. Phys. 16 (2014) 19917, http://dx.doi.org/10.1039/C4CP03113J.

[42] I. Wacławska, M. Szumera, J. Sułowska, Structural characterization of zinc-modified glasses from the SiO$_2$-P$_2$O$_5$-K$_2$O-CaO-MgO system, J. Alloys Compd. 666 (2016) 352–358, http://dx.doi.org/10.1016/j.jallcom.2016.01.125.

[43] S.P. Valappil, D. Ready, E.A. Abou Neel, D.M. Pickup, W. Chrzanowski, L.A. O'Dell, R.J. Newport, M.E. Smith, M. Wilson, J.C. Knowles, Antimicrobial gallium-doped phosphate-based glasses, Adv. Funct. Mater. 18 (2008) 732–741, http://dx.doi.org/10.1002/adfm.200700931.

[44] H. Gao, T. Tan, D. Wang, Effect of composition on the release kinetics of phosphate controlled release glasses in aqueous

medium, J. Control. Release 96 (2004) 21–28, http://dx.doi.org/10.1016/j.jconrel.2003.12.030.

[45] P.Y. Shih, J.Y. Ding, S.Y. Lee, 31P MAS-NMR and FTIR analyses on the structure of CuO-containing sodium poly- and metaphosphate glasses, Mater. Chem. Phys. 80 (2003) 391–396, http://dx.doi.org/10.1016/S0254-0584(03)00098-1.

[46] K. Griebenow, C.B. Bragatto, E.I. Kamitsos, L. Wondraczek, Mixed-modifier effect in alkaline earth metaphosphate glasses, J. Non-Cryst. Solids 481 (2018) 447–456, http://dx.doi.org/10.1016/j.jnoncrysol.2017.11.041.

[47] T. Ma, A.P. Jivkov, W. Li, W. Liang, Y. Wang, H. Xu, X.A. Han, Mechanistic model for long-term nuclear waste glass dissolution integrating chemical affinity and interfacial diffusion barrier, J. Nucl. Mater. 486 (2017) 70–85, http://dx.doi.org/10.1016/j.jnucmat.2017.01.001.

[48] C.A. Utton, R.J. Hand, P.A. Bingham, N.C. Hyatt, S.W. Swanton, S.J. Williams, Dissolution of vitrified wastes in a high-pH calcium-rich solution, J. Nucl. Mater. 435 (2013) 112–122, http://dx.doi.org/10.1016/j.jnucmat.2012.12.032.

[49] P. Pascuta, M. Bosca, G. Borodi, I. Vida-Simiti, E. Culea, Thermal, structural and magnetic properties of some zinc phosphate glasses doped with manganese ions, J. Alloys Compd. 509 (2011) 4314–4319, http://dx.doi.org/10.1016/j.jallcom.2011.01.056.

[50] L. Montagne, G. Palavit, R. Delaval, Effect of ZnO on the properties of (100−x)NaPO$_3$-xZnO glasses, J. Non-Cryst. Solids 223 (1998) 43–47, http://dx.doi.org/10.1016/S0022-3093(97)00444-4.

[51] D.R. Lide, CRC Handbook of Chemistry and Physics: A Ready-Reference Book of Chemical and Physical Data, CRC Press, Boca Raton, 2004.

[52] K.V. Shah, M. Goswami, S. Manikandan, V.K. Shrikhande, G.P. Kothiyal, Surface degradation behaviour of sodium borophosphate glass in aqueous media: some studies, Bull. Mater. Sci. 32 (2009) 329–336, http://dx.doi.org/10.1007/s12034-009-0047-3.

[53] C. Christoph Stähli, M.S. Mohammadi, K.E. Waters, S.N. Nazhat, Characterization of aqueous interactions of copper-doped phosphate-based glasses by vapour sorption, Acta Biomater. 10 (2014) 3317–3326, http://dx.doi.org/10.1016/j.actbio.2014.03.015.

[54] N. Papadopoulos, C.A. Drosou, Influence of weather conditions on glass properties, J. Univ. Chem. Technol. Metall. 47 (2012) 429–438.

[55] A. Tamayo, R. de la Torre, O. Ruiz, P. Lozano, M.A. Mazo, J. Rubio, Application of a glass fertilizer in sustainable tomato plant crops, J. Sci. Food Agric. 98 (2018) 4625–4633, http://dx.doi.org/10.1002/jsfa.8992.

[56] T. Labbilta, M. Ait-El-Mokhtar, Y. Abouliatim, M. Khouloud, A. Meddich, M. Mesnaoui, Innovative formulations of phosphate glasses as controlled-release fertilizers to improve tomato crop growth, yield and fruit quality, Molecules 26 (2021) 3928, http://dx.doi.org/10.3390/molecules26133928.

[57] J. Rubio, R. Rodríguez, A. Ciruelos, O. Ruiz, P.A. Lozano, R. De La Torre, New glass fertilizer for tomato crops to reduce environmental impact, Acta Hortic. 1159 (2017) 65–72, http://dx.doi.org/10.17660/ActaHortic.2017.1159.10.

[58] N.H. Abou-Baker, M. Ouis, M. Abd-Eladl, Appraisal of agriglass in promoting maize production under abiotic stress conditions, Silicon 10 (2018) 1841–1849, http://dx.doi.org/10.1007/s12633-017-9684-0.

[59] P.S. Bindraban, C.O. Dimkpa, R. Pandey, Exploring phosphorus fertilizers and fertilization strategies for improved human and environmental health, Biol. Fertil. Soils 56 (2020) 299–317, http://dx.doi.org/10.1007/s00374-019-01430-2.

[60] M. Ait-El-Mokhtar, T. Labbilta, M. Anli, A. Boutasknit, Y. Abouliatim, M. Khouloud, M. Mesnaoui, A. Meddich, Phosphate glass-based controlled-release fertilizers improve wheat growth, yield and grain nutritional quality under field conditions, Gesunde Pflanzen. (2022) 1–13, http://dx.doi.org/10.1007/s10343-022-00647-w.

[61] M. Adnan, M. Hussain, M.Z. Anjum, F.U. Rehman, H.B. Bilal, M.D. Toor, R. Ahmad, Role of phosphorous in wheat production: a review, Int. J. Agric. Sci. 8 (2020) 10–15.

[62] M. Ait-El-Mokhtar, M. Baslam, R. Ben-Laouane, M. Anli, A. Boutasknit, T. Mitsui, S. Wahbi, A. Meddich, Alleviation of detrimental effects of salt stress on date palm (*Phoenix dactylifera* L.) by the application of arbuscular mycorrhizal fungi and/or compost, Front. Sustain. Food Syst. 4 (2020) 131, http://dx.doi.org/10.3389/fsufs.2020.00131.

[63] M. Ion, A. Şerdinescu, L. Pîrcălabu, M. Sava, Use of vitreous fertilizers with slow release of nutrients in viticulture, Curr. Trends Nat. Sci. 1 (2012) 101–106.

[64] H. Liu, C.Y. Shi, H. Zhang, Z.Z. Wang, S. Chai, Effects of potassium on yield, photosynthate distribution, enzymes' activity and ABA content in storage roots of sweet potato (*Ipomoea batatas* Lam.), Aust. J. Crop Sci. 7 (2013) 735–743.